Proceedings of Global Power and Propulsion Society
ISSN-Nr: 2504-4400
GPPS Hong Kong 2023
October 17-19, 2023
www.gpps.global

GPPS-TC-2023-0015

BLADE EXCITATION RELATED FLOW BEHAVIOR ANALYSIS ON THE TURBOCHARGER'S CENTRIFUGAL COMPRESSOR WITH VOLUTE AND CASING TREATMENT

Xuedong Zheng
Institute for aero engine Tsinghua University
zhengxd21@mails.tsinghua.edu.cn

Baotong Wang
Institute for aero engine Tsinghua University
wangbaotong@tsinghua.edu.cn

Chuanxiang Yan
Institute for aero engine Tsinghua University
yancx20@mails.tsinghua.edu.cn

Xinqian Zheng
State Key Lab of Automotive Safety & Energy Tsinghua University
zhengxq@tsinghua.edu.cn

Beijing, China

ABSTRACT

High cycle fatigue due to unsteady aerodynamic excitation is a common failure mode of turbocharger blades. This paper numerically investigates the flow unsteady characteristic in a turbocharger compressor with asymmetric volute and SRCT(Self-recirculation-Casing-Treatment). Unsteady-Reynolds-Averaged-Navier-Stokes (URANS) computation is performed on the full-annulus compressor model. The data-driven method of Dynamic Mode Decomposition (DMD) is used to explore the unsteady flow behavior related to blade excitation, also the result is compared with Fourier Decomposition (FD) method. It is concluded that asymmetric volute is a strong excitation source, which forms the 1Nodal Diameter(ND) and 2ND pressure pattern. As the operating condition changes from choke side to near-stall side with back pressure increasing, 1ND morphs into 2ND. The SRCT is a complex excitation source that contains two dominant phenomena caused by the potential field and the interaction between injection flow and the mainstream of the blades. The SRCT should be carefully designed to alleviate the injecting flow non-uniformity caused by the strut. As for the comparison of DMD and FD, the result from DMD is very similar to that from FD in the analysis of periodic unsteady flow characteristics, and both of them can reveal the blade excitation source to support the further blade design.

INTRODUCTION

Turbocharger plays an important role in the operation of an internal combustion engine with downsizing the engine and improving the fuel economy. Rotating at a high speed, the compressor of a turbocharger boosts the air pressure to a higher level, thus improving the cycle parameter including the air flow rate and pressure. However, the environment the compressor works in is very complicated, featuring high flow unsteadiness.

The resonance induced by flow unsteadiness can cause high cycle fatigue(HCF) of the compressor blade, threatening the safety of the system. Thus, it is indispensable to analyze the unsteadiness excitation source and avoid resonance(or high response level) during the design or operating stage for a turbocharger compressor. Ordinary sources of unsteadiness are from the geometry characteristics of the compressor (blades, asymmetric volute, vane diffusor, casing treatment). In principle, the flow unsteadiness in the compressor can be categorized into the following types:

1)Potential field disturbance or circumferential acoustic wave caused by the relative motion of equally spaced blade-vane-strut and other asymmetry geometry(Ernst et al., 2011; Li., 2016): Essentially this type of unsteadiness features the pressure wave in the view of linearized flow assumption, and it can travel up-downstream in the flow passage and sometimes reflect from the structure because of its "acoustic wave" characteristic. Besides the excitation, this type of unsteadiness is also the source of the noise. (Broatch et al., 2016)

2)Wake of the upstream geometry(Hilbert et al., 1997, El-Aini et al., 1997): Essentially this type of unsteadiness is the entropy/vortex wave in the view of linearized flow assumption, which only travels downstream. The wake is the main cause of the HCF according to the literature(El-Aini et al., 1997).

3)Flow instability: this type of unsteadiness mainly includes the well-known rotating stall and surge(Semlitsch., 2016). It always manifests as a systematically nonlinear behavior due to its close relationship to the geometry design concept and the working condition of the whole machine. This unsteadiness is devastating to the structure's integrity. Fortunately, unlike the previous types of unsteadiness, flow instability can be avoided by carefully selecting the design operating point of the machine.

In reality, these types of unsteadiness always interact with each other, which means that these sources do not only solely excite the wheel blade, but the interaction between them can induce extra excitation sources. What's more, the significance of these excitations also varies with the operating conditions, which makes it more difficult to predict vibration using the traditional method (Campbell Diagram, especially high-order modes). Thus it is important to deeply understand the mechanism and strength of different types of flow unsteadiness and their interaction in the compressor to support the blade reliability design.

Traditionally, Fourier decomposition(FD) is used to clarify the frequency characteristic of flow unsteadiness. Recently, the dynamic mode decomposition(DMD)(Schmid., 2010) method is getting popular, which can be regarded as an extension of FD. The DMD can not only extract the frequency character, but it can also capture the dominant spatial flow pattern or spatial relationship of the whole flow field, especially for the aperiodic flow behavior. Based on these temporal-spatial patterns, one can explore underlying mechanisms to build the Reduced-Order Model (ROM) of the original system. This method has been used for the post-processing of experimental measurement and numerical results of unsteady flow fields such as the tip vortex structure, rotating stall, or surge(Semlitsch., 2016; Yang et al ., 2021). However, few previous study focuses on the use of DMD in the excitation analysis as far as the authors know.

In this paper, a turbocharger centrifugal compressor, which manifests as the damage of the leading edge of several main blades is taken as the research object. There is no evidence of the impeller blade rubbing at the casing. Therefore, HCF induced by blade vibration may be the root of the leading edge failure. The centrifugal compressor uses a vane-less diffusor, inlet casing bleed system with 6 struts, which introduces potential and wake unsteadiness. As the first step to reveal the blade failure mechanisms and avoid the HCF of the compressor blade, all the unsteady exciting sources should be recognized and analyzed, which is the intention of this work. In this paper, the authors utilize the DMD methods to diagnose the underlying excitation sources that could cause the failure of the compressor blade based on the unsteady computational fluid dynamics (CFD)results and compared the results of DMD with that of FD. First, the unsteady flow field is calculated using the full-annular model at three representative operating conditions from three rotating speeds. Then, the post-processing by using the DMD is conducted. Finally, the unsteady pressure field is decomposed into multiple unsteady pressure modes by DMD, and the flow mechanisms behind these modes related to blade excitation are discussed and analyzed.

METHODOLOGY

Turbocharger Compressor in Study

The case studied here is a typical automobile turbocharger compressor shown in Figure 1. It comprises the volute with a vaneless diffuser, the blade wheel, and the back seal plate. The blade wheel has 7 main blades and 7 splitters, which are made of 2A70 aluminum alloy. The rated speed of the wheel is 75000RPM, and the maximum speed is 82000RPM. Near the axial position of the inducer tip, there is a bleed casing treatment system with 6 struts supporting the structure to recirculate the low-momentum fluid to the upstream compressor inlet and enhance the stable working range.

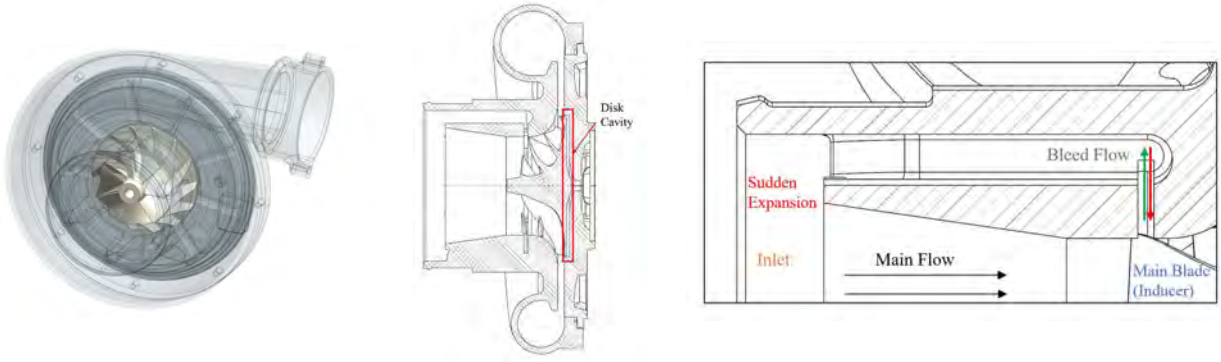

(a) 3D model (b) Cross Section of compressor (c) Cross Section of Bleed System

Figure 1 Model of the Compressor

The steady performance characteristic from the numerical simulation and experiment of the compressor is shown in Figure 2. The operating conditions including near choke, peak efficiency, and near stall at the rotating speed of 40000,

60000, and 75000RPM in Figure 2 marked by the red circles are chosen for further analysis. Moreover, the pressure ratio and mass flow rate corresponding to each operating condition are also illustrated in Table 1.

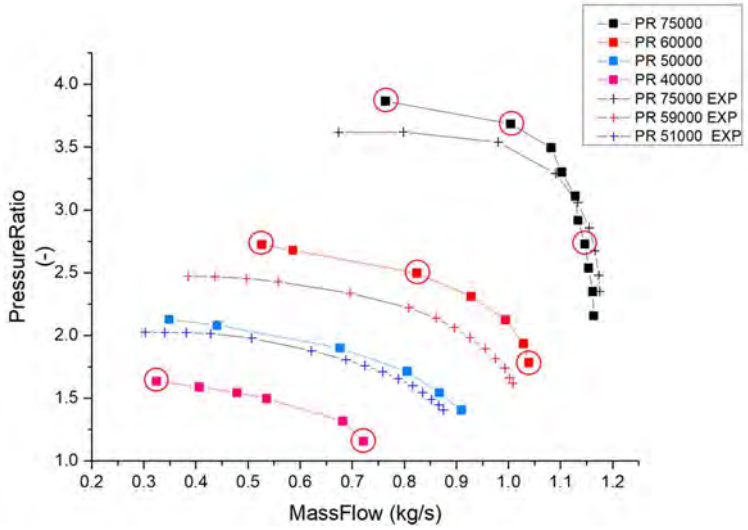

Figure 2 Map by Steady Computation and Experimental Data

Table 1 Working Condition In Analysis

Speed(RPM)	75000		60000		40000	
	Massflow(kg/s)	PR(-)	Massflow(kg/s)	PR(-)	Massflow(kg/s)	PR(-)
Choke	1.147	2.73	1.039	1.79	0.721	1.16
MaxEff	1.004	3.69	0.824	2.50	0.479	1.54
Stall	0.741	3.92	0.527	2.73	0.324	1.63

CFD Method

The commercial code ANSYS-CFX, which is widely used in the field of turbomachinery, is utilized for CFD computation.

In order to obtain the unsteady flow field for further DMD analysis, the Unsteady Reynolds-Averaged Navier-Stokes (URANS) equations are solved in the flow passage of the compressor. The second-order backward Euler scheme is used in this paper for temporal discretization, which is an implicit scheme with second-order accuracy. As for the spatial discretization of convective terms, this paper adopts the High-Resolution interpolation method, which realizes second-order accuracy while keeping stability. The Shear Stress Transportation (SST) turbulent model proposed by Menter(1994) is chosen for the turbulence closure, which is considered to be capable of dealing with the large pressure gradients flow accurately, compared to other engineering turbulence models. Besides the unsteady simulation, the steady simulation is also conducted to obtain a steady performance as shown in Figure 2.

Figure 3 shows details of the mesh. The simulation domain is discretized using the hybrid mesh. Due to the complex geometry, the flow domain of the casing treatment and volute are mainly discretized by the tetrahedral mesh. As the key component, the impeller domain is fully discretized by the hexahedral mesh. In CFX topology setting, the meshes are all treated as unstructured finite-volume mesh. The fillet in the hub and tip clearance are also considered in the numerical model. The number of mesh for each component is listed in Table 2.

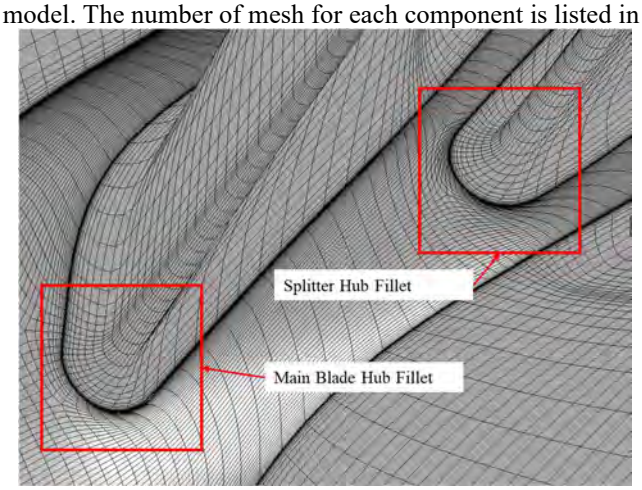

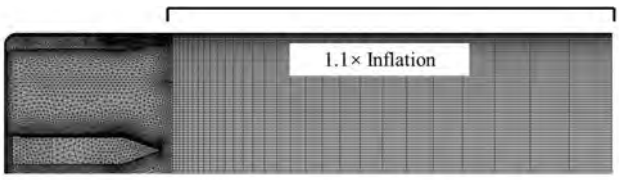

(a) Mesh at Hub Fillet

(b) Mesh at Inlet Duct and Bleed System
Inlet coarsening Ratio~1.1

Figure 3 Mesh for the Numerical Simulation

Table 2 Mesh Number of Each Component

	Bleed System	Blade Wheel	Volute
Node Number	2.75M	5.05M	0.25M
Element Number	5.50M	4.49M	0.69M

For mesh near the wall boundary, y+<10 is ensured by resolving the boundary layer, and y+ near the impeller blade surfaces is less than 2, especially. To remove the non-physical reflection caused by the reflecting boundary, the mesh of the inlet domain is gradually coarsened to damp out the acoustic along the axial direction. Meanwhile, the 1D non-reflection boundary is chosen for further reduction of acoustic reflection.

For the unsteady simulation, the full annulus model consisting of the bleed system, blade wheel, and volute is used. All rotor-stator interfaces are treated as sliding interfaces. As for time step setup, the time step independency study has been conducted on the full annular model at the operating condition with rotating speed and pressure ratio equal to 75000RPM and 3.7, respectively. 5, 10, 20, and 40 steps per blade passage (big-big blade passage)rotation are chosen to conduct the unsteady simulation and compare the pressure results. Finally, 20-steps per blade passage is chosen.

In order to validate the numerical method, as shown in Figure 2, the performance map is compared with the experimental result. At the rotating speed of 75000RPM. the numerical result well captures the choke mass flow rate and the trend of pressure ratio change with the variation of mass flow rate. At the near stall condition, the pressure ratio is overestimated by the numerical simulation, which is quite common in the numerical simulation of centrifugal compressors at high-speed conditions. The neglecting of the impeller disk cavity(Figure 1(b)) could be the main reason contributing to this discrepancy (Qiao, B et al., 2023). Though the discrepancy in performance, the acoustic wave in the cavity is thought to be neglectable. The fundamental acoustic resonance frequency is estimated according to the analytical equation by Rona,(2007):

$$f = \frac{a}{2\pi}[(\frac{\zeta}{R})^2 + (\frac{n\pi}{D})^2]^{0.5} \qquad (1.1)$$

where f, a, ζ, n, R, D are eigenfrequency, speed of sound, solution of eigen equation of cylinder mode, circumferential mode number, cavity radians, and cavity depth respectively. Substituting R, D, a, ζ , and n into 0.065m, 0.003m, 340m/s, 1.2556, and 14 (blade number) from the previous literature (Rona.,2007), the frequency can be obtained to be 80,470Hz, which is much higher than blade passing frequency 17500Hz at 75000RPM. Thus the impact of the cavity on acoustic excitation will not be considered here. According above discussion, the present numerical method is considered to fulfill the requirement of the research objective.

Dynamic Mode Decomposition (DMD) Method

Originating from Schmid(2010), the data-driven DMD method has been used and improved. The basic formulation of DMD is described as follows:

The unsteady properties in a high-dimensional system can be arrayed in a matrix form as follows.

$$V_1^N = [v_1, v_2, ..., v_n], V_2^N = [v_2, v_3, ..., v_{n+1}] \quad (1.2)$$

subscript indicates the time instance. The information of the system is contained in the matrix. Then according to Koopman's theory, a high dimensional(theoretically infinite dimensional, to capture the nonlinear behavior) operator A can be defined, which drives the system evolute with the time step. Using the A operator, the sampling can be related with:

$$v_{i+1} = Av_i \qquad (1.3)$$

As discussed, an operator A is a high-dimension operator, it is difficult to find A directly. Singular Value Decomposition(SVD) can be used in the DMD method to find a low-rank, low-order approximation of A .

$$V_1^N \approx U\Sigma W \qquad (1.4)$$

$$\tilde{A} = U^H V_2^N W^H \Sigma^{-1} = U^H A U \qquad (1.5)$$

Thanks to the similarity transformation, $\tilde{A}$ has the same eigenvalue as A . Finally by adopting the eigenvector matrix of $\tilde{A}$ and V_2^N , one can reconstruct the eigenvector ϕ of the matrix A , and the system vector can be expressed as:

$$v_k = \sum_{j=1}^{r} a_j \phi_j \lambda_j^{\,k} \quad (1.6)$$

Where ϕ_j is the j^{th} mode and λ_j is the corresponding eigenvalue of the mode. The mode frequency can be defined by:

$$f_j = \log(\lambda_j) / \Delta t \quad (1.7)$$

Where Δt is the sampling interval.

Finally, to evaluate the significance of the modes, modal energy (Broatch., 2019) is defined as follows:

$$E_j = \sum_{j=1}^{r} | a_j \lambda_j^{\,j-1} | \left\| \Phi_j \right\|^2 \Delta t \quad (1.8)$$

It should be noted that for a pure periodic system, the output of DMD mode reduces to a linear Fourier decomposition(FD) as discussed in(Chen et al.,2012) and the result of this paper verifies this feature(in the section *Overview of result*). Thus DMD can be seen as an extension of FD. However, DMD can deal with an aperiodic system and gives the trend of the mode. Another advantage of DMD is that it can capture low-frequency mode without "spectral leakage" which is common in FD. Although DMD and its variant are still subject to the Nyquist frequency constraint, there is no theoretical lower bound on the frequencies they can compute(Chen et al.,2012). Therefore, the windowing process is not necessary for the DMD analysis anymore. This has been verified by Ludewig (2022) using experimental data.

In this paper, the effect of the unsteady field on the impeller blade vibration is focused. Therefore, the unsteady pressure from the surfaces of all the blades including the main blade and splitter are sampled and the time series of pressure are used as input of DMD. To clarify the impact of SRCT and asymmetric volute, four planes are placed perpendicular to the axis, at the position of the inlet, chamber of the bleed groove, the bleed groove, and the outlet of the wheel. These planes and their numbers are shown in Figure 4 from P1 to P4. The sampling rate in time is chosen as 20 BPF (main blade passing frequency), the same as the computational time step, which also satisfies the Nyquist limitation.

(a) Computational Domains (b) Sampling Surfaces

Figure 4 Location of Sampling Surface

RESULTS AND DISCUSSION

Overview of result

The results of DMD can be interpreted from different points of view: energy spectrum, frequency components, and pressure spatial modes. The energy of mode, defined as formula(1.7), is a measurement of the mode significance, and a high mode energy represents the strong blade oscillation in the corresponding mode. The modal energies on the main blade are plotted against the relative frequency defined by "Engine Order"(EO),(EO=Frequency/RPS) at the rotating speed of 75000RPM in Figure 5 (a). The 0EO mode is the one that represents the steady pressure. The non-zero mode represents the unsteadiness with the frequency of EO×RPS. It can be observed that there are many energy peaks locating at the 1EO,2EO,6EO,12EO, and 18EO corresponding to the existence of significant unsteadiness due to the interaction between the blade with the volute and the struct, etc.

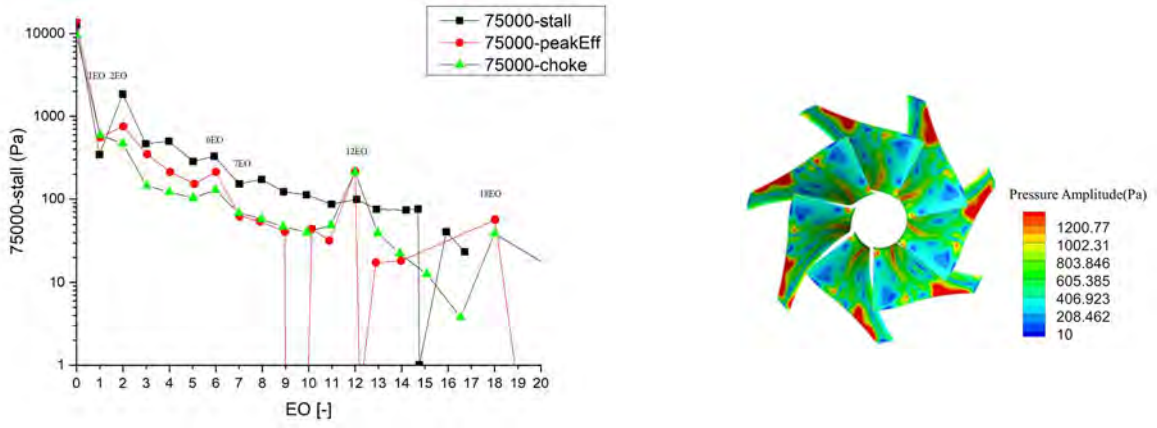

(a) Energy Spectrum Featuring Several Peaks

(b) Pressure Mode at 6EO Showing A "Nodal Diameter" Spatial Pattern

Figure 5 Energy Spectrum and Example Contour of Pressure Modes (Main Blade@75000RPM&PR3.69)

The DMD mode is defined as the pressure amplitude distribution of a certain frequency An example of the pressure mode contour of important interaction is shown in Figure 5 (b). The pressure amplitude of the mode indicates the fluctuation of the pressure. The larger the amplitude, the stronger the pressure fluctuation. In the next section, the typical types of unsteadiness in the energy spectrum will be discussed in detail.

Figure 6 shows the pressure mode on the main blades of the same frequency(6EO in Figure 5(a)) from the DMD and FD results. For FD, there is no windowing process and the pressure sampling rate is the same as that of DMD. Similar to the definition of DMD mode, the FD mode is also defined as the pressure amplitude distribution of a certain frequency. It can be observed that the two methods give almost the same result, the error between the two methods is less than 1%, which can be considered to be a verification of the theory(Chen et al.,2012).

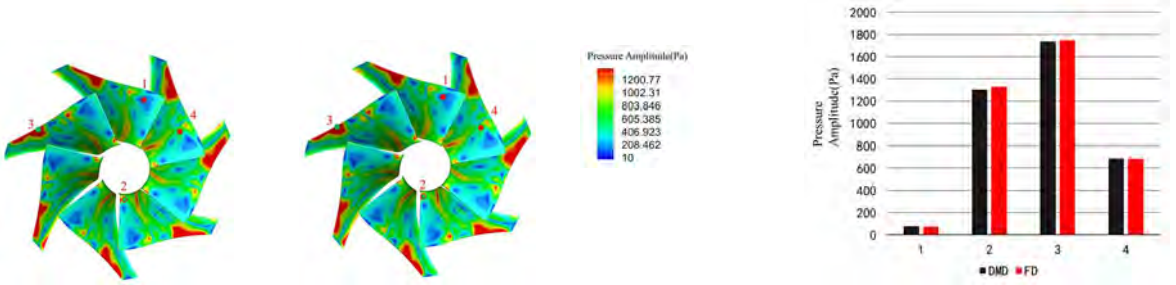

(a)DMD Mode (b)FD Mode (c)Pressure Amplitude on Sampling Point

Figure 6 Comparison of The Result between DMD and FD

Effect of Asymmetric volute.

In the centrifugal compressor, it is well-known that the strong flow unsteadiness can be induced by the volute asymmetry. Intuitively, the volute asymmetry imposes a once-per-revolution excitation on the blades which will induce 1EO vibration of the blade. As Figure 5(a) shows, one interesting phenomenon is that there are 2-3EO excitations that vary with the change in back pressure. As the pressure ratio increases, the 2 EO component is increasing such that the energy is more than that of 1EO(figure 5a). Such a result can also be observed on the splitter blade.

To further investigate this phenomenon, the 0EO pressure distribution in the diffuser and volute is shown in Figure 8. At the high back pressure(BP) operating conditions marked in Figure 7, the pressure contour of unsteady CFD shows a 2-lobe pattern with two pressure peaks along the circumferential direction. The difference of circumferential positions between two low-pressure regions(lobes) is around 180 degrees, one of the low-pressure regions is located around 60 degrees upstream of the volute tongue along the circumferential position. This pattern morphs into a mainly once-per-rev pattern at low BP conditions.

Similar results are reported by other authors(Niu et al.,2022). The 2-lobe pattern near the stall operating condition is considered to be the result of unsteady interaction between the blade wheel and volute asymmetry. This can be verified through the steady result with the mixing plane interface. The steady simulation result with a mixing plane interface at the impeller outlet is shown in Figure 9. The mixing plane interface treatment averages the parameter through the impeller outlet circumferentially (nevertheless the sliding interface transfer data directly). Thus the volute feels a uniform inlet

condition, and in Figure 9, there is only 1ND pattern which is induced by volute asymmetry. The only reason for the formation of the 2ND pattern is due to the interaction during the impeller passing through the sliding interface in the unsteady simulation.

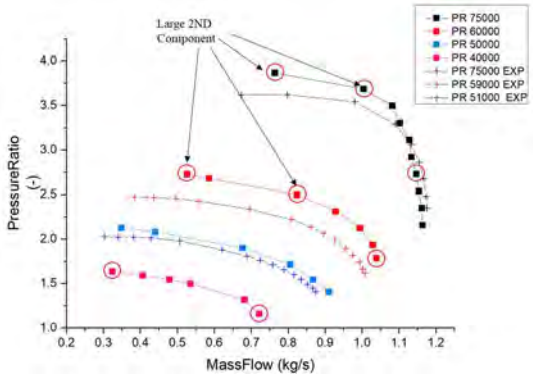

Figure 7 Working Conditions With Large 2ND Excitation

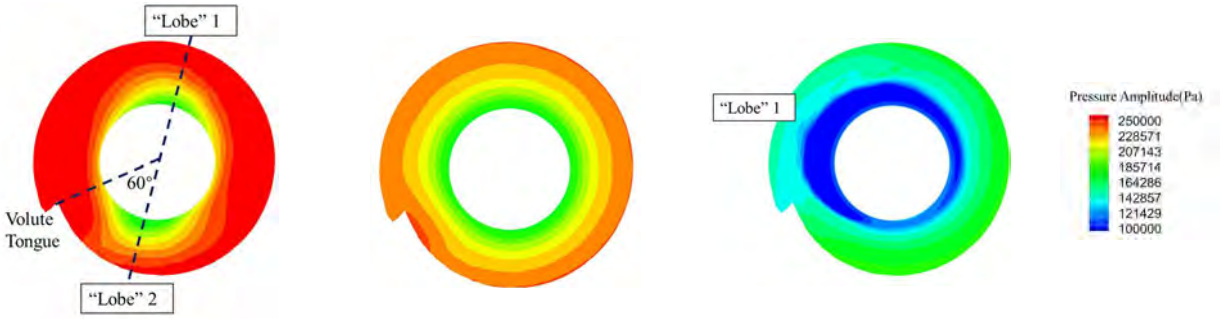

(a) 60000RPM&Stall (b) 60000 RPM &Peak Eff (c) 60000 RPM &Choke

Figure 8 0 Frequency Components of 60000RPM on Plane4(Volute)

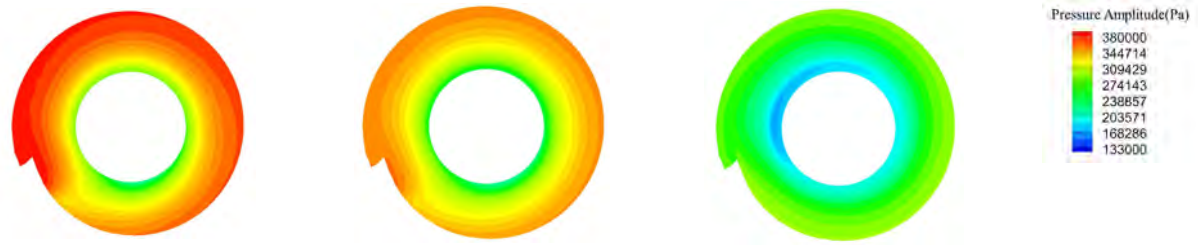

(a) 60000RPM&Stall (b) 60000RPM&Peak Eff (c) 60000RPM&Choke

Figure 9 Steady State CFD Pressure Results on Plane4(Volute) with Mixing Plane Interface

This phenomenon makes the excitation more complex as the working condition changes. When avoiding Campbell diagram crossing, the designer should give more concern on the 2EO excitation induced by the mentioned 2ND pattern. Moreover, the influences induced by volute asymmetry to the flow can propagate the upstream location. Figure 10 shows that the 7EO unsteady modes(excited by the main blade) in the P1 plane are distorted in phase with volute asymmetric pattern, which means that the pressure fluctuations at certain circumferential locations are higher than other ones. This can be explained by the change of blade load: as the blade passes the low-pressure region in volute, the blade load is reduced so the mass flow in this passage is increased and induces a pressure redistribution to influence the upstream flow field. This observation implies that some struct may fail faster than others due to the uniformity of excitation strength along the circumferential direction and should be considered in the structure design stage.

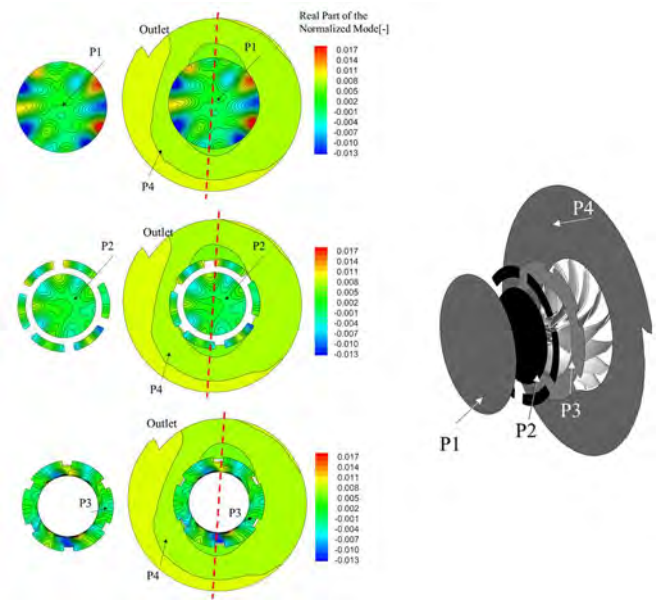

Figure 10 The Distortion Induced by Volute Influencing 7EO modes Upstream

Effect of bleed cavity strut

Another peak in the energy spectrum is 6EO and 12EO as shown in Figure 5(a), coinciding with the number of struts and twice of them. In the paper, the author calls this frequency as Strut Passing Frequency (SPF) in the rotor frame of reference. The 6^{th} and 12^{th} excitation introduce 1ND and 2ND aliasing circumferential modes on the blade wheel respectively.

Figure 11 shows the real part of the normalized mode of 6EO mode on the main blade surfaces. There are some global characteristics of the pressure mode: First, the 1ND aliasing pattern can be observed, which can be explained by the sampling theory; Second, at the locations of the bleed slot and passage shock wave, the gradient in the contour is larger than that at others. This large gradient indicates the shock wave is influenced by the existence of bleed system in Figure 11 (75000-270/75000-370).

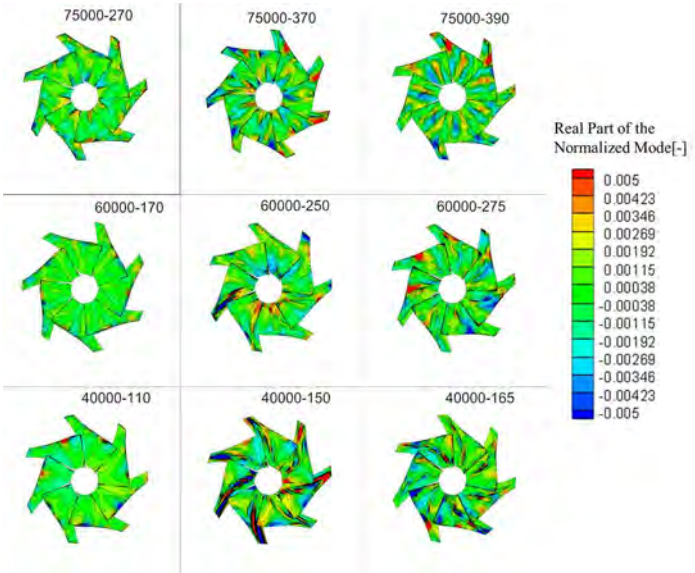

Figure 11 6EO Modes on Main Blade at Different Conditions

From the energy spectrum (Figure 5(a)), it can be observed that the energy of 12EO mode is more obvious at the low BP conditions than that at the high BP conditions and is in the same order as the 6EO mode magnitude, which means the influence of the strut is increasing with the decrement of back pressure. Figure 12 compares the energy ratio of 12EO and 6EO in the different operating conditions. Though the trend of energy ratio change seems not to be monotonous at the

rotating speed of 60000rpm, the ratio near the choke condition is clearly higher than that near the stall condition. This can be explained by the changed flow behavior in the bleeding cavity at different operating conditions.

At the low BP operating condition, the flow is injected into the blade passage through the slots. Therefore, the unsteady pressure change consists of two aspects: the pressure wave by strut potential flow and the interaction between the flow of blade passage and the injection flow stream. On the other hand, at the high BP operating conditions, the low momentum fluid near the blade tip region is intaken through the slots and recirculates in the bleed system, thus the second contribution of the situation in the low BP condition is caused by the interaction between the injection and main passage flow disappears. The flow behavior mentioned above can also be understood from the steady-state axial velocity contour as shown in Figure 13.

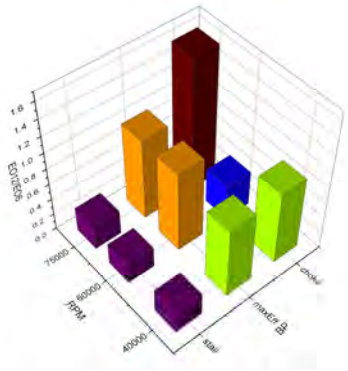

Figure 12 6EO Modes on Main Blade at Different Conditions

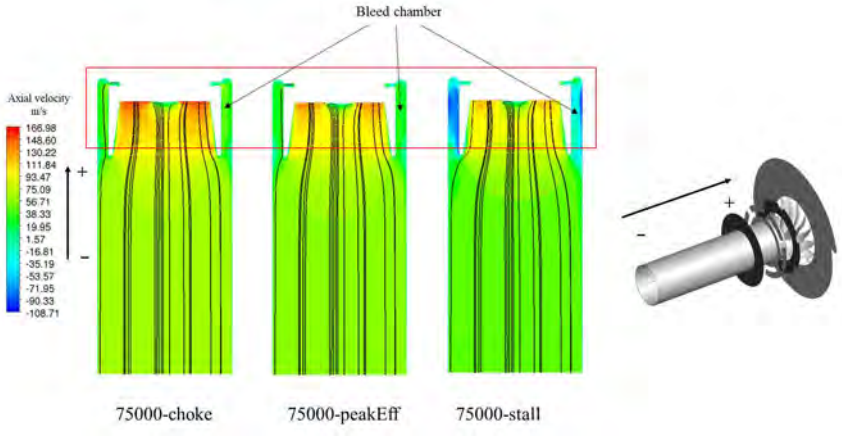

Figure 13 Axial FLOW Velocity in Bleed System

CONCLUSIONS

This paper investigates the unsteady flow characteristics and reveals the main excitation source for HCF in a turbocharger compressor with SRCT. The unsteady CFD is conducted at the different operating conditions (with changed speed and back pressure) by solving the URANS equations, the DMD post-processing method is employed to explore the dominant flow characteristics, and is compared with FD .The typical flow unsteady characteristics closely related to blade excitation are evaluated by the energy spectrum and mode contour results. The key conclusions can be drawn as follows:

1. For a periodic unsteady flow, the DMD method gives very similar result as FD method both in mode amplitude and frequency of dominant flow behavior.

2. For the studied centrifugal compressor consisting of impeller wheel, volute and SRCT, the frequency that should be considered when constructing the Campbell diagram for blade vibration design are RF, 2×RF, SPF, and 2×SPF. These frequencies are closely related to two types of blade excitation sources due to the unsteady flow: asymmetric volute, bleed cavity strut excitation.

3. The Asymmetric volute will excite 1ND and 2ND blade excitation patterns, the latter will appear in the high back pressure operating conditions. The effect of pressure distortion caused by the volute can propagate upstream to the inlet of the compressor, which imposes the excitation on the upstream component.

4. The excitation induced by the bleed cavity struts will change with the variation of working conditions. At the near stall conditions, the excitation is small and mainly features a frequency of SPF; At the near choke conditions, the excitation increases and mainly features 2×SPF. These phenomena highly depend on the flow behavior in the bleed cavity system.

In the future, the structure analysis should be performed and the mode force should be calculated as the next step of the present work.

ACKNOWLEDGMENTS

The authors want to appreciate Dr. Lou Fangyuan for his advice on the analysis of unsteady flow phenomena.

NOMENCLATURE

a	Speed of Sound	R	Radians
ζ	Solution of Eigen Equation of Cylinder Mode	n	Circumferential Mode Number
D	Depth of Back Cavity	v_k	Sampling Quantity Vector at Time Instance *k*
V_k^N	Matrix By N Sampling Quanitiy Vectors	$A / \tilde{A}$	LinearOperator/Truncated Linear Operator
U / W	Orthogonal Matrix in Singular Value Decomposition	$\sum$	Singular Value Matrix
Φ_j	The *j*th Mode	a_j	Amplitude of *j*th Mode
f_j	Frequency of *j*th Mode	Δt	Sampling Time Interval
E_j	Energy of *j*th Mode	λ_j	Eigen Value of *j*th Mode

ABBREVIATIONS

BPF	Blade passing frequency	RPS	Revolution Per Second
DMD	Dynamic Mode Decomposition	SPF	Strut Passing Frequency
FD	Fourier Decomposition	PR	Pressure Ratio
HCF	High Cycle Fatigue	SRCT	Self-recirculation Casing Treatment
RPM	Revolution Per Minute		

References

Broatch, A., García-Tíscar, J. O. R. G. E., Roig, F., & Sharma, S. (2019). Dynamic mode decomposition of the acoustic field in radial compressors. Aerospace Science and Technology, 90, 388-400 ,https://doi.org/10.1016/j.ast.2019.05.015.

Chen, K. K., Tu, J. H., & Rowley, C. W. (2012). Variants of dynamic mode decomposition: boundary condition, Koopman, and Fourier analyses. Journal of nonlinear science, 22, 887-915, https://doi.org/10.1007/s00332-012-9130-9

Ernst, M., Michel, A., & Jeschke, P. (2011). Analysis of rotor-stator-interaction and blade-to-blade measurements in a two stage axial flow compressor.

El-Aini, Y., deLaneuville, R., Stoner, A., Capece, V., El-Aini, Y., deLaneuville, R., . & Capece, V. (1997, July). High cycle fatigue of turbomachinery components-Industry perspective. In 33rd joint propulsion conference and exhibit (p. 3365).

Hilbert, G. R., Ni, R. H., & Takahashi, R. K. (1997, November). Forced response prediction of gas turbine rotor blades. In ASME International Mechanical Engineering Congress and Exposition (Vol. 18350, pp. 491-498). American Society of Mechanical Engineers, https://doi.org/10.1115/IMECE1997-0750

Holmes, M., Gray, A., & Isbell, C. (2007, December). Fast SVD for large-scale matrices. In Workshop on Efficient Machine Learning at NIPS (Vol. 58, pp. 249-252).

Li, J. (2016). Multi-Row Aerodynamic Interactions and Mistuned Forced Response of an Embedded Compressor Rotor (Doctoral dissertation, Duke University).

Ludewig, A., Brenner, G., & Skinder, K. (2022, June). DMD Analysis of Radial Turbomachinery. In Turbo Expo: Power for Land, Sea, and Air (Vol. 86021, p. V005T10A014). American Society of Mechanical Engineers.

Menter, F. R. (1994). Two-equation eddy-viscosity turbulence models for engineering applications. AIAA journal, 32(8), 1598-1605.

Niu, Z., Sun, Z., Wang, B., & Zheng, X. (2022). Effects of nonaxisymmetric volute on rotating stall in the vaneless diffuser of centrifugal compressors. Journal of Engineering for Gas Turbines and Power, 144(5), 051015.

Qiao, B., He, X., Vahdati, M., Ju, Y., & Zhang, C. On the Over-Prediction of Centrifugal Compressor Pressure Ratio in the High Impeller Tip Mach Number Regime.

Rona, A. (2007). The acoustic resonance of rectangular and cylindrical cavities. Journal of Algorithms & Computational Technology, 1(3), 329-356.

Schmid, P. J. (2010). Dynamic mode decomposition of numerical and experimental data. Journal of fluid mechanics, 656, 5-28, doi:10.1017/S0022112010001217

Semlitsch, B., & Mihăescu, M. (2016). Flow phenomena leading to surge in a centrifugal compressor. Energy, 103, 572-587.

Vahdati, M., Simpson, G., & Imregun, M. (2011). Mechanisms for wide-chord fan blade flutter. Journal of Turbomachinery, 133(4).

Yang, C., Fu, L., Hu, C., & Shi, X. (2021). Modeling and dynamic mode analysis of compressor impeller spike-type stall with global stability approach. International Journal of Mechanical Sciences, 201, 106486.,https://doi.org/10.1016/j.ijmecsci.2021.106486.